

# Skyrme-Random-Phase-Approximation description of E1 strength in $^{92-100}\text{Mo}$

J. Kvasil, P. Vesely

*Institute of Particle and Nuclear Physics,*

*Charles University,*

*CZ-18000 Praha, Czech Republic;*

*kvasil@ipnp.troja.mff.cuni.cz*

V.O. Nesterenko, W. Kleinig \*

<sup>1</sup> *Bogoliubov Laboratory of Theoretical Physics,*

*Joint Institute for Nuclear Research,*

*Dubna, Moscow region, 141980, Russia;*

*nester@theor.jinr.ru*

P.-G. Reinhard

*Institut für Theoretische Physik II, Universität Erlangen, D-91058, Erlangen, Germany*

S. Frauendorf †

*Institut für Strahlenphysik, Forschungszentrum,*

*Rossendorf, D-01314, Dresden, Germany*

(Dated: May 26, 2018)

## Abstract

The isovector dipole E1 strength in  $^{92,94,96,98,100}\text{Mo}$  is analyzed within the self-consistent separable random-phase approximation (SRPA) model with Skyrme forces SkT6, SkM\*, SLy6, and SkI3. The special attention is paid to the low-energy region near the particle thresholds (4-12 MeV), which is important for understanding of astrophysical processes. We show that, due to a compensation effect, the influence of nuclear deformation on E1 strength below 10-12 MeV is quite modest. At the same time, in agreement with previous predictions, the deformation increases the strength at higher energy. At 4-8 MeV the strength is mainly determined by the tail of E1 giant resonance. The four Skyrme forces differ in description of the whole giant resonance but give rather similar results below 12 MeV.

---

\* Permanent address: Tech. Universität Dresden, Inst. für Analysis, D-01062, Dresden, Germany.

† Present address: Department of Physics, University of Notre Dame, Indiana, 46556, USA.

## I. INTRODUCTION

The isovector giant dipole resonance (GDR) remains to be a subject of intense study, now with the accent to exotic nuclei and astrophysical problems [1]. Besides the GDR is actively used for inspection and upgrade of the modern self-consistent mean-field approaches [2, 3], e.g. those based on Skyrme forces [4, 5].

In this paper we will investigate GDR in a chain of even-mass isotopes  $^{92-100}\text{Mo}$ . This chain is of particular interest because here we have photoabsorption experimental data not only above but also below the particle emission thresholds, down to 4 MeV [6, 7]. Being rather weak, the E1 strength near the thresholds is however important for understanding astrophysical processes, e.g. of the stellar photodisintegration rate [8, 9, 10]. In principle, this strength should depend on such factors as nuclear size and deformation. Since the chain  $^{92-100}\text{Mo}$  involves spherical ( $A=92,94,96$ ) and deformed ( $A=98,100$ ) nuclei [11], it is suitable for estimation of both factors.

The E1 strength in the molybdenum chain has been recently explored in the random-phase-approximation (RPA) with the phenomenological Nilsson [12] and Woods-Saxon [7] single-particle potentials. In both cases, the important role of the deformation was found. Namely, it was predicted that prolate/triaxial deformation significantly increases the E1 strength at 10-14 MeV. However, the calculations [7, 12] are not self-consistent and so an additional analysis within more involved microscopic models is desirable. In the present paper we explore the dipole strength in  $^{92-100}\text{Mo}$  in the framework of the self-consistent separable RPA (SRPA) with Skyrme forces [13, 14, 15]. SRPA covers both spherical [13] and deformed [15, 16, 17] and so is the proper tool for the present analysis. Factorization of the residual interaction minimizes the computational effort and therefore allows the systematic exploration. The model was already used for the analysis of the GDR in different mass regions, including drip line and superheavy nuclei [17, 18]. Note that unlike the previous Skyrme-RPA studies of the low-energy E1 strength [10], where the GDR deformation splitting was introduced phenomenologically, SRPA treatment of the deformation effects is fully self-consistent.

We will show that conclusions [7, 12] on the impact of nuclear deformation should be amended in the sense that the result strictly depends on the energy region. Namely, the deformation indeed increases the E1 strength at  $E > 10-12$  MeV but, at the same time, has a minor impact at lower energy, i.e. near the particle thresholds. The later is caused by a compensation effect of the GDR branches. This effect is quite general and becomes apparent just in the low-energy regions of astrophysical interest.

## II. CALCULATION SCHEME AND GROUND STATE PROPERTIES

The calculations are performed within SRPA [13, 14, 15] with the representative set of Skyrme forces, SkT6 [19], SkM\* [20], SLy6 [21], and SkI3 [22]. These forces expose a variety of features (effective masses, etc) relevant for the GDR [2, 3, 17]. Amongst them, the force SLy6 provides the best compromise for the description of the GDR in heavy nuclei [15, 17, 18]. The SRPA residual interaction involves contributions from the time-even densities (nucleon  $\rho$ , kinetic  $\tau$  and spin-orbital  $\vec{\mathfrak{S}}$ ), time-odd current  $\vec{j}$ , direct and exchange Coulomb terms, and pairing (with delta forces at the BCS level) [13, 14, 15, 18].

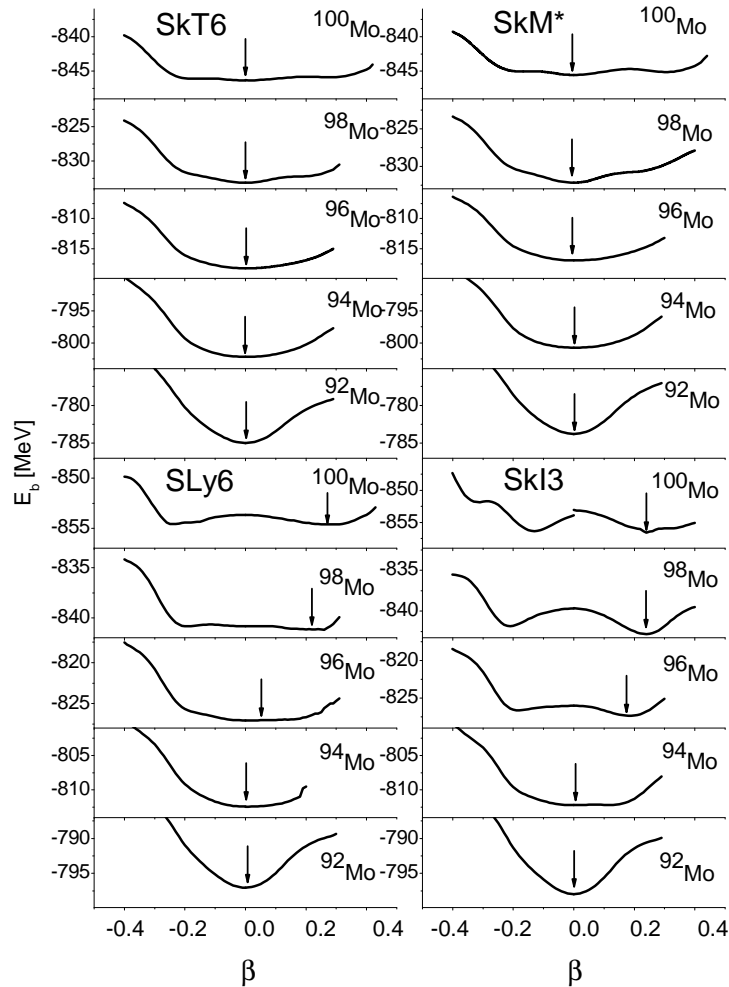


FIG. 1: Energy surfaces (= binding energies) in Mo isotopes, obtained in quadrupole-constrained mean-field calculations with Skyrme forces SkT6, SkM\*, SLy6, and SkI3. The equilibrium axial deformations  $\beta$  are indicated by arrows.

TABLE I: Experimental thresholds for  $(\gamma, n)$ ,  $(\gamma, p)$ ,  $(\gamma, 2n)$ ,  $(\gamma, np)$ , and  $(\gamma, 2p)$  reactions [23] and equilibrium deformations  $\beta$  calculated with the forces SkT6, SkM\*, SLy6, and SkI3 in  $^{92-100}\text{Mo}$ .

A	Thresholds (MeV)					$\beta$			
	$E_n$	$E_p$	$E_{2n}$	$E_{np}$	$E_{2p}$	SkT6	SLy6	SkM*	SkI3
92	12.7	7.5	22.8	19.5	12.6	0.0	0.0	0.0	0.0
94	9.7	8.5	17.7	17.3	14.5	0.0	0.0	0.0	0.0
96	9.2	9.3	16.5	17.8	16.1	0.0	0.05	0.0	0.18
98	8.6	9.8	15.5	17.9	17.2	0.0	0.22	0.0	0.24
100	8.3	10.1	14.2	18.0	19.5	0.0	0.27	0.0	0.24

The axial equilibrium quadrupole deformation

$$\beta = \sqrt{\frac{\pi}{5}} \frac{1}{Z \langle r^2 \rangle_p} \int d\vec{r} \rho_p(\vec{r}) r^2 Y_{20} \quad (1)$$

(where  $\rho_p(\vec{r})$  is the proton density in the ground state and  $\langle r^2 \rangle_p = \int d\vec{r} \rho_p(\vec{r}) r^2 / Z$  is the r.m.s. proton radius) is determined by minimization of the total energy, see Fig. 1 and Table I. As is seen from Fig. 1, the nuclei  $^{94-100}\text{Mo}$  are soft to  $\beta$ , especially the heavy isotopes. Partly this is because of their transition character. Besides,  $^{98}\text{Mo}$  and  $^{100}\text{Mo}$  are probably triaxial (with  $\epsilon_2 = 0.18, \gamma = 37^\circ$  and  $\epsilon_2 = 0.21, \gamma = 32^\circ$ , respectively [11, 12]). In the present study the triaxiality is omitted, which may also lead to a wide plateau and local minima for  $\beta < 0$ . Altogether, there is appreciable ambiguity in determination of the equilibrium deformation  $\beta$ . In  $^{98,100}\text{Mo}$  we see a significant variation of  $\beta$  with the Skyrme force. While SkT6 and SkM\* favor a spherical shape (in contradicts with significant  $\epsilon_2$  in Refs. [11, 12]), the forces SLy6 and SkI3 give more reasonable results. So just SLy6 and SkI3 will be mainly used in the further analysis of the deformation effects. Note, that triaxiality can cause an additionally spread of the E1 strength. In the present study this effect is masked by the proper Lorentz smoothing of the strength.

The photoabsorption (in mb) is computed as [24]

$$\sigma_\gamma(E) = 4.01 E S(E) \quad (2)$$

where

$$S(E) = \sum_{\mu=0,1} \sum_{\nu} E_\nu |\langle \Psi_\nu | \hat{f}_{E1\mu} | \Psi_0 \rangle|^2 \zeta(E - E_\nu) \quad (3)$$

is the strength function with the Lorentz weight  $\zeta = \Delta / (2\pi[(E - E_\nu)^2 + \Delta^2/4])$  and isovector transition operator  $\hat{f}_{E1\mu} = N/A \sum_{p=1}^Z r_p Y_{1\mu}(\Omega_p) - Z/A \sum_{n=1}^N r_n Y_{1\mu}(\Omega_n)$ . In Eq. (3),  $E_\nu$  and  $\Psi_\nu$  mark eigenvalue and eigenfunction of  $\nu$ -th RPA state, and  $\Psi_0$  is the ground state eigenfunction.

The summation runs over the RPA spectrum until  $E_{cut} = 45$  MeV. The Lorentz function with the averaging parameter  $\Delta$  is used to simulate the broadening effects beyond SRPA (triaxiality, escape widths, and coupling with complex configurations). Besides, this smoothing allows to avoid unnecessary details of the calculated strength which in any case are not resolved in experiment. Following [15, 17, 18], the averaging  $\Delta=2$  MeV is optimal. SRPA allows a direct computation of the strength function (without finding the manifold of RPA states), which greatly reduces the effort.

The calculations use a large basis space of single-particle states, from the bottom of the potential well up to  $\sim +16$  MeV. The integral photoabsorption

$$\Sigma = \int_0^{E_{cut}} dE \sigma_\gamma(E) \quad (4)$$

exhausts up to 98% of the energy-weighted sum rule  $EWSR = 9(\hbar e)^2/(8\pi m_1^*) \cdot NZ/A$  with the isovector effective mass  $m_1^*$  arising due to the velocity-dependent densities  $\tau$ ,  $\vec{\mathfrak{S}}$ , and  $\vec{j}$  [17, 25]. So our basis is indeed large enough to explore the GDR. The EWSR should not be confused with the Thomas-Reiche-Kuhn (TRK) sum rule  $\Sigma_{TRK} = 60NZ/A$  mb MeV which deals with the bare nucleon mass  $m$ .

### III. RESULTS AND DISCUSSION

Results of the calculations for E1 strength are given in Figs. 2-7.

In Figs. 2 the photoabsorption in semimagic spherical  $^{92}\text{Mo}$  is presented. The logarithmic scale is used for a convenient comparison with the experimental data. Different smoothing parameters  $\Delta$  are used. It is seen that the most appropriate agreement with experiment takes place for  $\Delta=1$  and 2 MeV, especially in the low-energy 4-12 MeV of our interest (the same for other isotopes  $^{94-100}\text{Mo}$ ). Taking also into account our previous results for the GDR [15, 17, 18], we chose for the further analysis  $\Delta=2$  MeV. As is seen from Fig. 2, for this averaging we generally reproduce the GDR energy and width. At the same time, the calculated  $\sigma_\gamma(E)$  systematically exceeds the experimental data at the GDR top and falls short at its right flank. This discrepancies can be partly caused by omitting the complex configurations. Being included, those configurations could redistribute the strength from the middle to the right side of the GDR, thus improving agreement with the experiment. Besides, the discrepancy at the GDR top can be also an artifact of the comparison of the calculated photoabsorption with the separate  $(\gamma, p)$  and  $(\gamma, xn)$  channels.

In the logarithmic scale the photoabsorption obtained for different Skyrme forces looks rather

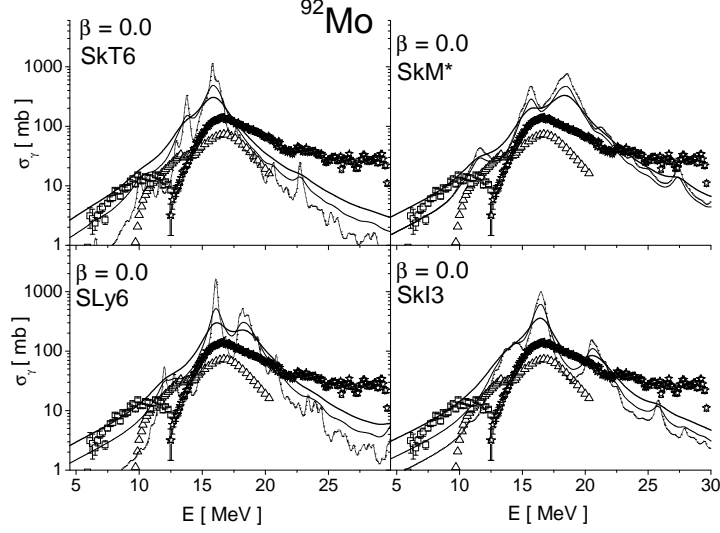


FIG. 2: Photoabsorption (in logarithmic scale) in  $^{92}\text{Mo}$  calculated with Skyrme forces SkT6, SkM\*, SLy6, and SkI3 with the averaging  $\Delta=0.25$  MeV (dotted curve), 1 MeV (solid curve) and 2 MeV (bold solid curve). The experimental  $(\gamma, \gamma')$ ,  $(\gamma, p)$ , and  $(\gamma, xn)$  data [6, 7] are given by boxes, triangles, and stars in the energy intervals 5.1-12.5, 7.9-20.3, and 12.4-29.7 MeV, respectively.

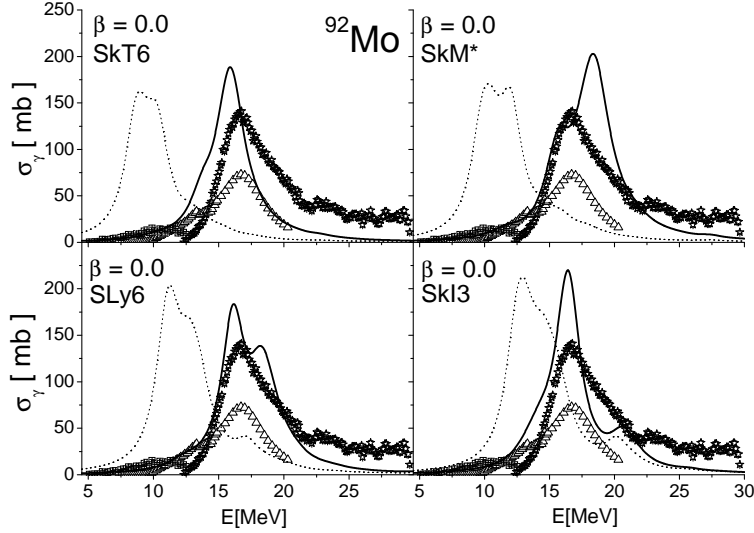


FIG. 3: The same as in Fig. 2 but for linear scale and averaging  $\Delta=2$  MeV only. The dash curve exhibits the unperturbed two-quasiparticle (2qp) results.

similar. To distinguish the difference between predictions of different forces, one should switch to the linear scale, which is done in Figs. 3 and 4 for semimagic  $^{92}\text{Mo}$  and deformed  $^{100}\text{Mo}$ . Now it is seen that in spherical  $^{92}\text{Mo}$  the best description is for SLy6. For deformed  $^{100}\text{Mo}$  only SLy6 and SkI3 results are presented. The forces SkT6 and SkM\* predict for  $^{100}\text{Mo}$  the spherical shape and so obviously fail here. The calculations for  $^{100}\text{Mo}$  overestimate the experimental data (as photoabsorption over  $(\gamma, xn)$ ) but keep EWSR and provide an acceptable agreement for the GDR

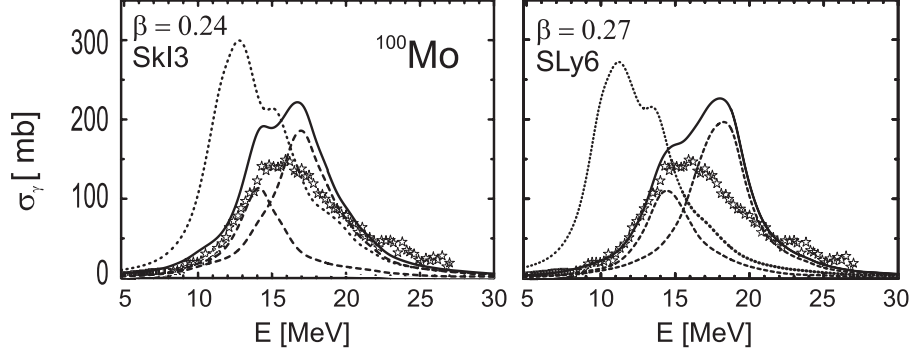


FIG. 4: The same as in Fig. 3 for  $^{100}\text{Mo}$  and forces SLy6 and SkI3. The experimental data [6, 7] for  $(\gamma, \gamma')$  at 4.1-8.1 MeV and  $(\gamma, xn)$  at 8.3-27 MeV are given by boxes and stars, respectively. The GDR branches  $\mu = 0$  (small bump) and  $\mu = 1$  (twice larger bump) exhibited by the dash curve demonstrate the deformation splitting of the resonance.

energy centroid and width.

As was mentioned in the introduction, the E1 strength near the particle thresholds is of particular interest for some astrophysical problems [8, 9]. In this connection, it is important to understand the main physical mechanisms responsible for the evolution of this strength with the neutron number  $N$  in the isotope chain. First of all, this evolution is determined by the empirical rule  $E_{GDR} = 81A^{-1/3}$  MeV [24] relating the GDR energy and nuclear mass number  $A$ . The higher  $N$  (and so  $A$ ), the more the GDR downshift and stronger the GDR tail (and relevant E1 strength) near the thresholds. This size factor seems to dominate. However, two other effects, nuclear deformation and internal E1 strength in the region (pygmy resonance), can also come to play and influence the general size trend.

These effects are inspected in Figs. 5-7. The impact of deformation is illustrated in Fig. 5, where the E1 strength calculated at zero and non-zero deformations is compared with the experimental data [6, 7]. We get the nonzero deformation only in  $^{98}\text{Mo}$  and  $^{100}\text{Mo}$  for the forces SLy6 and SkI3. In all other cases the calculations give  $\beta=0$ , see Table 1. Fig. 5 shows that for  $\beta=0$  all the forces provide more or less acceptable agreement with the experiment, the best for SkT6 and SkI3. Inclusion of the deformation changes the results. While at  $E > 12$  MeV we have, in accordance with Refs. [7, 12], increasing E1 strength, in the interval of our main interest,  $E < 12$  MeV, we see its modest decrease. The effect is prominent and even stronger than the change in E1 strength for the neighbor isotopes.

The deformation effect for  $E < 12$  MeV can be explained (for both prolate and oblate shapes) by destructive competition of two factors, deformation shifts of  $\mu = 0$  and  $\mu = 1$  branches of the

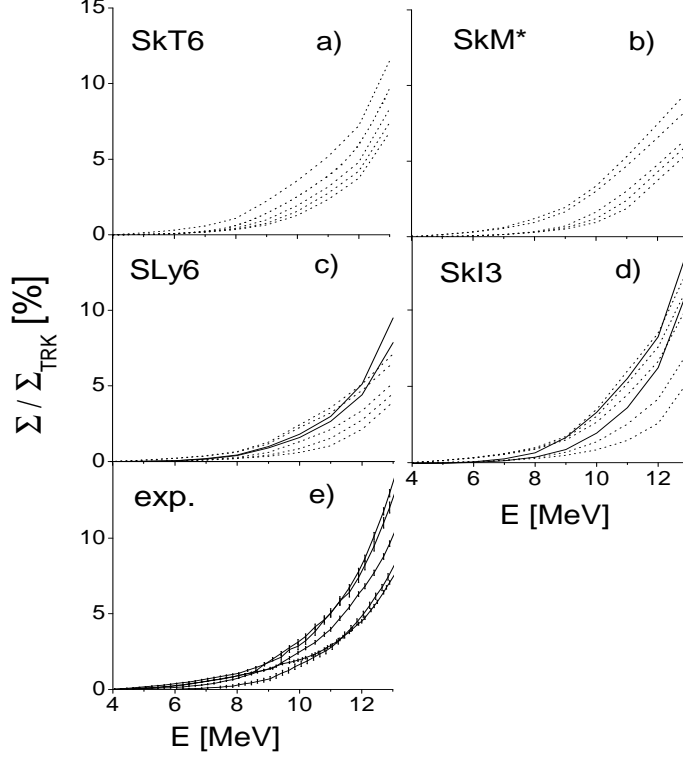


FIG. 5: The calculated a)-d) and experimental [6, 7] e) integral low-energy photoabsorption in Mo isotopes. The calculated results are exhibited for non-zero (= equilibrium in  $^{98,100}\text{Mo}$  for SLy6 and SkI3) and zero (= equilibrium in other cases) deformations by solid and dotted curves, respectively. In all the panels the sequence of curves for  $^{92,94,96,98,100}\text{Mo}$  has the same order: from the lowest for  $^{92}\text{Mo}$  to the highest for  $^{100}\text{Mo}$ .

GDR. Indeed, the deformation shifts the GDR branches in opposite directions thus minimizing the resulting deformation impact. Though the branch  $\mu = 1$  is twice stronger than  $\mu = 0$  one, its deformation shift is less, hence a strong mutual compensation of both  $\mu = 0$  and  $\mu = 1$  deformation impacts. Being strong, the compensation is usually not complete. So, depending on the concrete case, one may finally observe a modest decrease or increase of the low-energy E1 strength. Of course, the compensation holds at the energies far enough from the lower GDR branch (which is just the case for  $E < 12$  MeV). Instead, while approaching the lower GDR branch, we always gain E1 strength with the deformation, as was earlier found in Refs. [7, 12].

These arguments are illustrated in Fig. 6 for prolate  $^{100}\text{Mo}$ . The calculations were done for SLy6 with averaging parameters  $\Delta = 2$  and 1 MeV. It is seen that for  $\Delta = 2$  the deformation-induced  $\mu = 0$  and 1 contributions indeed strictly compensate each other, thus leading to a slight decrease of E1 strength at  $9 < E < 12$  MeV and no effect at the lower energy. Instead, in accordance with [7, 12], the strength grows at  $E > 12$  MeV. The minor deformation effect at  $9 < E < 12$  MeV

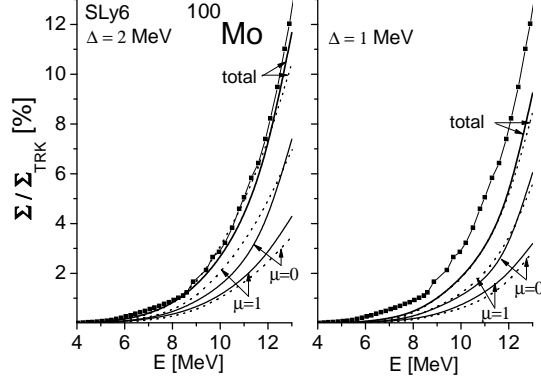


FIG. 6: The low-energy photoabsorption in  $^{100}\text{Mo}$ , calculated with the force SLy6 for  $\beta = 0$  (dotted curves) and equilibrium deformation  $\beta = 0.27$  (solid curves). The averaging  $\Delta = 2$  MeV (left) and 1 MeV (right) is used. The total strength as well as the strengths of the branches  $\mu = 0$  and  $\mu = 1$  are indicated by arrows. The experimental data [6, 7] are depicted by full boxes.

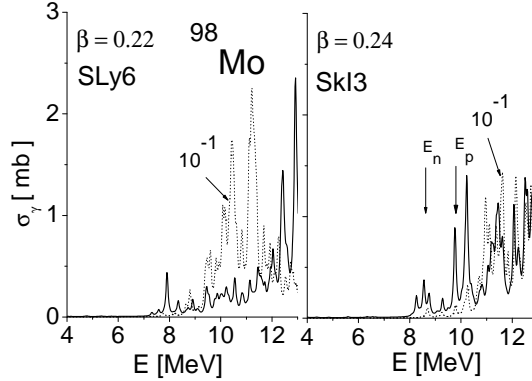


FIG. 7: The low-energy photoabsorption in deformed  $^{98}\text{Mo}$ , calculated for the forces SLy6 and SkI3 with (solid curve) and without (dash curve) the residual interaction. To see the fine structure, the small averaging  $\Delta = 0.1$  MeV is used. The unperturbed photoabsorption is decreased 10 times as indicated. The vertical arrows show  $(\gamma, n)$  and  $(\gamma, p)$  thresholds.

becomes invisible for the less averaging  $\Delta = 1$  MeV, which is explained by weakening the GDR low-energy tail. Note that for  $\Delta = 2$  MeV we get much better agreement with the experiment than for  $\Delta = 1$  MeV, which additionally justifies the large averaging as the best choice.

Finally, Fig. 7 demonstrates for deformed  $^{98}\text{Mo}$  the role of internal E1 excitations in forming the low-energy strength. To make visible a fine structure, the small averaging  $\Delta = 0.1$  MeV is used. It is seen that for both forces the E1 strength between 4 and 7-8 MeV does not exhibit any internal structure while the structure at 7-9 MeV is weak. So, the E1 strength for  $E < 9$  MeV is mainly determined by the GDR tail (the same for other Mo isotopes). This means that all the effects discussed above for the GDR are indeed relevant for the energies near and below the particle

thresholds. The absence of E1 structures at 4-8 MeV is natural since 2qp excitations with  $\Delta\mathcal{N}=1$  ( $\mathcal{N}$  is a principle shell quantum number) lie at a higher energy, see Figs. 3 and 4. Note that for  $E > 9 - 10$  MeV the E1 strength rises and exhibits more appreciable structure (perhaps the pygmy resonance observed in [6]).

#### IV. SUMMARY

The E1 strength in  $^{92,94,96,98,100}\text{Mo}$  is investigated in the framework of the self-consistent separable RPA method for the set of Skyrme forces SkT6, SkM\*, SLy6, and SkI3. The main attention is paid to low-energy strength below the particle thresholds, which is of a keen interest for astrophysical problems [8, 9]. To our knowledge, this is the first Skyrme-RPA study of E1 strength in Mo isotopes with the self-consistent treatment of deformation effects. Some important factors (triaxiality, coupling with complex configurations, escape widths) are simulated by the Lorentz smoothing and others (pairing impact, energy dependence of the smoothing) need an additional analysis, which makes our description of E1 strength yet tentative. Nevertheless, some useful conclusions can be done.

We confirmed our previous statement [15, 16, 17, 18] that the force SLy6 with the Lorentz smoothing  $\Delta = 2$  MeV gives the most reasonable description of the whole GDR. The low-energy E1 strength is shown to be mainly determined by the GDR tail. In spherical  $^{92,94,96}\text{Mo}$ , this strength is well described by all the forces.

It is found that the deformation impact in the low-energy E1 strength depends on the particular energy interval. While approaching the GDR,  $E > 12$  MeV, we get a definite increment of the strength with the deformation (as was earlier found in Refs. [7, 12]). However, at  $E < 12$  MeV, i.e. near and below the particle thresholds, the deformation impact almost vanishes because of the compensation of the deformation contributions from  $\mu = 0$  and  $\mu = 1$  GDR branches. The effect of triaxiality should still be checked. We plan to extend our exploration to Nd and Sm isotope chains where the triaxiality is absent.

#### Acknowledgments

We thank Prof. F. Dönau for initiation of this work and fruitful discussions. The work was partly supported by the DFG grant RE 322/11-1 and grants Heisenberg - Landau (Germany - BLTP JINR) and Votruba - Blokhintsev (Czech Republic - BLTP JINR) for 2008 year. W.K. and

P.-G.R. are grateful for the BMBF support under contracts 06 DD 139D and 06 ER 808. This work is also a part of the research plan MSM 0021620859 supported by the Ministry of Education of the Czech Republic. It was partly funded by Czech grant agency (grant No. 202/06/0363) and grant agency of Charles University in Prague (grant No. 222/2006/B-FYZ/MFF).

---

- [1] K. Langanke and M. Wiescher, *Rep. Prog. Phys.* **64**, 1657 (2001).
- [2] M. Bender, P.-H. Heenen, and P.-G. Reinhard, *Rev. Mod. Phys.* **75**, 121 (2003).
- [3] J.R. Stone and P.-G. Reinhard, *Prog. Part. Nucl. Phys.* **58**, 587 (2007).
- [4] T.H.R. Skyrme, *Phil. Mag.* **1**, 1043 (1956).
- [5] D. Vauterin and D.M. Brink, *Phys. Rev.* **C5**, 626 (1972).
- [6] G. Rusev, E. Grosse, M. Erhard, A. Junghans, K. Kosev, K.D. Schilling, R. Schwengner, and A. Wagner, *Eur. Phys. J.* **A27**, 171 (2006).
- [7] R. Schwengner, N. Benouaret, R. Beyer, F. Doenau, M. Erhardt, S. Frauendorf, E. Grosse, A. R. Junghans, J. Klug, K. Kosev, C. Nair, N. Nankov, G. Rusev, K. D. Schilling, and A. Wagner, *Nucl. Phys.* **A788**, 331c (2007); R. Schwengner, [www.fzd.de/FWK/MITARB/rs/TalkSNP2008.pdf](http://www.fzd.de/FWK/MITARB/rs/TalkSNP2008.pdf).
- [8] M. Arnold and S. Goriely, *Phys. Rep.* **384**, 1 (2003).
- [9] H. Utsunomiya, P. Mohr, A. Zilges, and M. Rayet, *Nucl. Phys.* **A777**, 459 (2006).
- [10] S. Goriely and E. Khan, *Nucl. Phys. A* **706**, 217 (2002).
- [11] G. Rusev, R. Schwengner, F. Dönaue, M. Erhardt, S. Frauendorf, E. Grosse, A. R. Junghans, L. Käubler, K. Kosev, L. K. Kostov, S. Mallion, K. D. Schilling, A. Wagner, H. von Garrel, U. Kneissl, C. Kohstall, M. Kreutz, H. H. Pitz, M. Scheck, F. Stedile, P. von Brentano, C. Fransen, J. Jolie, A. Linnemann, N. Pietralla, and V. Verner, *Phys. Rev.* **C73**, 044308 (2006).
- [12] F. Dönaue, G. Rusev, R. Schwengner, A. R. Junghans, K. D. Schilling, and A. Wagner, *Phys. Rev.* **C76**, 014317 (2007).
- [13] V.O. Nesterenko, J. Kvasil, and P.-G. Reinhard, *Phys. Rev.* **C66**, 044307 (2002).
- [14] V.O. Nesterenko, J. Kvasil, W. Kleinig, P.-G. Reinhard, and D.S. Dolci, [ArXiv: nucl-th/0512045](https://arxiv.org/abs/nucl-th/0512045).
- [15] V.O. Nesterenko, W. Kleinig, J. Kvasil, P.-G. Reinhard, and P. Vesely, *Phys. Rev.* **C74**, 054306 (2006).
- [16] V.O. Nesterenko, W. Kleinig, J. Kvasil, P. Vesely, and P.-G. Reinhard, *Int. J. Mod. Phys. E* **16**, 624 (2007).
- [17] V.O. Nesterenko, W. Kleinig, J. Kvasil, P. Vesely, and P.-G. Reinhard, *Int. J. Mod. Phys. E* **17**, 89, (2008).
- [18] W. Kleinig, V.O. Nesterenko, J. Kvasil, P.-G. Reinhard, and P. Vesely, *Phys. Rev.* **C78**, 044313 (2008).
- [19] F. Tondeur, M. Brack, M. Farine, and J.M. Pearson, *Nucl. Phys.* **A420**, 297 (1984).
- [20] J. Bartel, P. Quentin, M. Brack, C. Guet, and H.-B. Håakansson, *Nucl. Phys.* **A386**, 79 (1982).
- [21] E. Chabanat, P. Bonche, P. Haensel, J. Meyer, and R. Schaeffer, *Nucl. Phys.* **A627**, 710 (1997).

- [22] P.-G. Reinhard and H. Flocard, Nucl. Phys. **A584**, 467 (1995).
- [23] A.V. Varlamov, V.V. Varlamov, D.S. Rudenko and M.E. Stepanov, Atlas of Giant Resonances, INDC(NDS)-394, 1999.
- [24] P. Ring and P. Schuck, *The Nuclear Many-Body Problem* (Springer-Verlag, New York, 1980).
- [25] E. Lipparini and S. Stringari, Phys. Rep. **175**, 103 (1989).